Available online at www.sciencedirect.com
SCIENCE DIRECT
Journal of Catalysis 233 (2005) 41–50
JOURNAL OF CATALYSIS
www.elsevier.com/locate/jcat

Low-temperature oxidation of CO over $Pd/CeO_2–TiO_2$ catalysts with different pretreatments

Huaqing Zhu [a], Zhangfeng Qin [a], Wenjuan Shan [b], Wenjie Shen [b], Jianguo Wang [a,*]

[a] *State Key Laboratory of Coal Conversion, Institute of Coal Chemistry, Chinese Academy of Sciences, PO Box 165, Taiyuan, Shanxi 030001, PR China*
[b] *State Key Laboratory of Catalysis, Dalian Institute of Chemical Physics, Chinese Academy of Sciences, PO Box 110, Dalian, Liaoning 116023, PR China*

Received 27 January 2005; revised 13 April 2005; accepted 21 April 2005

Available online 23 May 2005

Abstract

A comprehensive study of the low-temperature oxidation of CO was conducted over Pd/TiO_2, Pd/CeO_2, and $Pd/CeO_2–TiO_2$ pretreated by a series of calcination and reduction processes. The catalysts were characterized by N_2 adsorption, XRD, H_2 chemisorption, and diffuse-reflectance infrared Fourier transform spectroscopy. The results indicated that $Pd/CeO_2–TiO_2$ has the highest activity among these catalysts, whether in the calcined state or in the reduced state. The activity of all of the catalysts can be improved significantly by the pre-reduction, and it seems that the reduction at low temperature (LTR, 150 °C) is more effective than that at high temperature (HTR, 500 °C), especially for Pd/CeO_2 and Pd/TiO_2. The catalysts with various supports and pretreatments are also different in the reaction mechanisms for CO oxidation at low temperature. Over Pd/TiO_2, the reaction may proceed through a surface reaction between the weakly adsorbed CO and oxygen (Langmuir–Hinshelwood). For Ce-containing catalysts, however, an alteration of reaction mechanism with temperature and the involvement of the oxygen activation at different sites were observed, and the light-off profiles of the calcined Pd/CeO_2 and $Pd/CeO_2–TiO_2$ show a distortion before CO conversion achieves 100%. At low temperature, CO oxidation proceeds mainly via the reaction between the adsorbed CO on Pd^0 sites and the lattice oxygen of surface CeO_2 at the Pd–Ce interface, whereas at high temperature it proceeds via the reaction between the adsorbed CO and oxygen. The high activity of $Pd/CeO_2–TiO_2$ for the low-temperature CO oxidation was probably due to the enhancements of both CO activation, caused by the facilitated reduction of Pd^{2+} to Pd^0, and oxygen activation, through the improvement of the surface oxygen supply and the oxygen vacancies formation. The reduction pretreatment enhances metal–support interactions and oxygen vacancy formation and hence improves the activity of CO oxidation.

Keywords: CO oxidation; Palladium; Ceria; Titania; Pretreatment; Calcination; Reduction; $CeO_2–TiO_2$

1. Introduction

The catalytic oxidation of CO at low temperature has attracted considerable attention because of its wide applications in exhaust abatement for CO_2 lasers, trace CO removal in enclosed atmospheres, automotive emission control, and CO preferential oxidation for proton exchange membrane fuel cells. Catalysts containing noble metals proved to be very effective for CO oxidation at low temperature. Among them, platinum and CeO_2 are two important components in the three-way catalysts for automobile exhaust purification [1,2], and supported Pd catalysts exhibit excellent activity for the low-temperature oxidation of CO and hydrocarbons compared with supported Pt and Rh catalysts [3].

After reduction at high temperature (about 500 °C), noble metals supported on reducible oxides such as TiO_2, CeO_2, and Nb_2O_5 may undergo a change in the metal–support interface due to the strong metal–support interaction (SMSI) effect [4,5]. The SMSI effect can be assessed through observation of the suppression of H_2 or CO chemisorption with reduction temperature, and with the help of certain probe reactions such as hydrogenation and hydrogenolysis [6–9].

The SMSI in M/TiO_2 after reduction at high temperature ($\geqslant$ 500 °C) has been attributed to both electronic and geo-

* Corresponding author. Fax: +86 351 4041153.
E-mail address: iccjgw@sxicc.ac.cn (J. Wang).

0021-9517/$ – see front matter
doi:10.1016/j.jcat.2005.04.033

metric effects (metal decorations) [4,5]. In contrast, different explanations are proposed for the SMSI in M/CeO_2: (1) an epitaxial growth of small noble metal particles on CeO_2; (2) alloy formation between noble metals and Ce [10,11]; (3) decoration or encapsulation of noble metals by partially reduced ceria [12–14]; and (4) pure electronic interactions [15,16].

In our previous work, Pd supported on ceria–titania mixed oxides prepared by sol–gel precipitation followed by supercritical fluid drying (SCFD) exhibited high activity for CO oxidation at low temperature [17]. Further work on temperature-programmed reduction (TPR) with H_2 and CO as reducing agents suggested that Pd–Ce interaction in Pd/CeO_2–TiO_2 favors the reduction of both PdO and CeO_2, which contributes to the high activity of CO oxidation at low temperature [18]. These works also suggested that the pretreatments of calcination and reduction may exhibit significant effects on the catalytic behavior of Pd/CeO_2–TiO_2.

The objective of this work is therefore to conduct a comprehensive study of the low-temperature oxidation of CO over Pd/TiO_2, Pd/CeO_2, and Pd/CeO_2–TiO_2 pretreated by a series of calcination and reduction processes. Through the light-off tests and various characterizations such as N_2 adsorption, XRD, H_2 chemisorption, and diffuse-reflectance infrared Fourier transform spectroscopy (DRIFTS), the catalytic activity was correlated with the conditions of the catalyst pretreatments, the state of the active Pd species, and the interaction between Pd and supports under the specific reaction conditions. Based on these examinations, the reaction mechanism for CO oxidation over the different catalysts was then proposed and used to explain these observations.

2. Experimental

2.1. Catalyst preparation

CeO_2, TiO_2, and CeO_2–TiO_2 supports were prepared by sol–gel precipitation followed by SCFD, and Pd-supported catalysts were prepared by incipient wetness impregnation with aqueous $PdCl_2$ solution as the Pd precursor, as described elsewhere [17,18]. The mole ratio of titania to ceria was 5 for the mixed CeO_2–TiO_2 support, and Pd loading was 1 wt% for the Pd-supported catalysts.

2.2. Catalytic tests and catalyst pretreatments

The catalytic oxidation of CO was carried out in a quartz tubular flow microreactor with an internal diameter of 6.0 mm at atmospheric pressure. About 200 mg catalyst of 40–60 mesh was used per run, as described previously [17]. The catalysts were first pretreated under an air flow (30 ml/min) at 500 °C for 1 h, followed by purging with argon flow (30 ml/min) at the same temperature for 1 h, and then the catalysts were cooled to room temperature under the argon flow. The catalysts in this stage are referred to as *calcined*. Further pretreatments included *reduction* with H_2 *at low temperature* (150 °C, LTR), *reduction at high temperature* (500 °C, HTR), and *re-oxidation* with air (500 °C, ReO). The catalysts were then purged with argon flow again for 2 h and cooled to room temperature with the protection of argon flow. After that, the catalysts were ready for the switch from inert gas flow to the reacting media.

The reacting stream consisted of 1.0% CO + 1.0% O_2 (by volume), balanced with argon and the space velocity was 39,000 ml g^{-1} h^{-1}. The reaction started immediately after the reacting stream entered the reactor at room temperature. After the reactivity at ambient temperature had reached a relatively steady level, the light-off test (temperature-programmed reaction) was conducted at a heating rate of 2 °C/min until CO was completely converted into CO_2. The produced CO_2 and unreacted CO were periodically analyzed on line with a gas chromatograph equipped with a 3 mm × 3 m stainless-steel column packed with carbon molecular sieve, a post-column methanator that converted CO and CO_2 into CH_4, and a flame ionization detector.

2.3. Catalyst characterization

2.3.1. Surface area and XRD

The surface area of the catalysts was measured by nitrogen adsorption at 77.4 K with ASAP2000 (Micromeritics Instrument Co. USA). The catalyst samples were degassed at 200 °C and 6.7 Pa for 4–5 h before the measurement.

XRD characterization was preformed on a Rigaku D/max-2500 X-ray diffraction spectrometer. The diffraction patterns were recorded at room temperature with Cu-K_α radiation (0.15418 nm, 40 kV, and 100 mA). The average crystallite size was determined from the diffraction peak broadening with the Scherrer formula [19].

2.3.2. Pd dispersion

Pd dispersion on the catalysts was determined by hydrogen–oxygen titration (HOT) in a multiple adsorption apparatus, TP 5000-II (Tianjin-Xianquan, China). The measurement was performed in a quartz microreactor with 50 mg sample in each run. The sample was first purified in an air flow at 500 °C for 1 h and purged with a nitrogen flow for 1 h. The pretreatments of the catalysts included LTR, HTR, and ReO + LTR processed in ways similar to what is described above. H_2 chemisorption (HC) was performed via an eight-port pulse valve at 25 °C, and the signal of H_2 in the outlet was detected with a thermal conductivity detector. The amount of irreversibly adsorbed H_2 was determined from the difference between the two adsorption processes. After the HC step, the catalyst sample was subjected to a successive O_2 titration (OT) and H_2 titration (HT). In the OT step, the sample was exposed to O_2 pulses to a saturated adsorption and then purged by nitrogen for more than 30 min. The HT procedure was similar to that for HC. Pd dispersion was calculated from the amount of irreversible H_2 uptake

that occurred in both HC and HT by assuming a ratio of H to Pd of 1, as described in the following sections.

2.3.3. DRIFTS

DRIFTS of CO adsorption was measured with a spectrometer Vector 22 (Bruker Optik) as described elsewhere [18]. To determine the initial states of Pd species, the spectra of CO adsorption at 25 °C were recorded after the sample was exposed to CO (5.01 vol%) in an argon flow for more than 30 min to a saturated adsorption and then purged with a helium flow for 15 min. The spectra of CO adsorption under reaction conditions were recorded as the sample was exposed to CO (1.05 vol%) + O_2 (1.01 vol%) in a nitrogen flow for about 30 min at each temperature. The measurements of catalysts after calcination, LTR, and HTR pretreatments (with 5.04 vol% H_2 in helium) were made in a similar way.

3. Results and discussion

3.1. Behaviors of CO oxidation at low temperature

To examine the effects of pretreatments on the reaction behaviors of different catalysts, CO oxidation was carried out at room temperature until the preliminary activity diminished to a stable value and thereafter with temperature programming at a heating rate of 2 °C/min until CO conversion reached 100%.

Comparisons of CO oxidation over Pd/CeO_2, Pd/TiO_2, and Pd/CeO_2–TiO_2 catalysts with different pretreatments (as calcined, after LTR or HTR) are shown in Fig. 1. For the catalysts after calcination, Pd/CeO_2–TiO_2 was much more active than Pd/TiO_2 and Pd/CeO_2. At ambient temperature, CO was completely converted to CO_2 over calcined Pd/CeO_2–TiO_2 (with a duration of about 45 min), and the conversion diminished gradually with time (about 90 min later), whereas the Pd/TiO_2 and Pd/CeO_2 catalysts showed very low activity for CO oxidation. The light-off profiles indicate that the temperatures needed for a complete CO conversion over calcined Pd/CeO_2, Pd/TiO_2, and Pd/CeO_2–TiO_2 were 204, 120, and 97 °C, respectively. It is interesting to note that the light-off profiles of the calcined Pd/CeO_2 and Pd/CeO_2–TiO_2 showed a distortion before CO conversion achieved 100%. The light-off profile of the calcined Pd/CeO_2 showed a plateau at 120–135 °C with a CO conversion of 65%, and that of Pd/CeO_2–TiO_2 gave a peak at 51 °C with a CO conversion of 65%.

The catalytic activity was promoted significantly by the reduction pretreatments, and LTR was more efficient than HTR, especially for Pd/CeO_2 and Pd/TiO_2. After the LTR pretreatment, the preliminary activity of the catalysts improved markedly at ambient temperature; complete CO conversion over the LTR-pretreated Pd/CeO_2–TiO_2 took about 100 min. The temperature required for a complete CO conversion over the LTR-pretreated Pd/CeO_2, Pd/TiO_2, and Pd/CeO_2–TiO_2 in the light-off tests also decreased to 97, 70, and 54 °C, respectively.

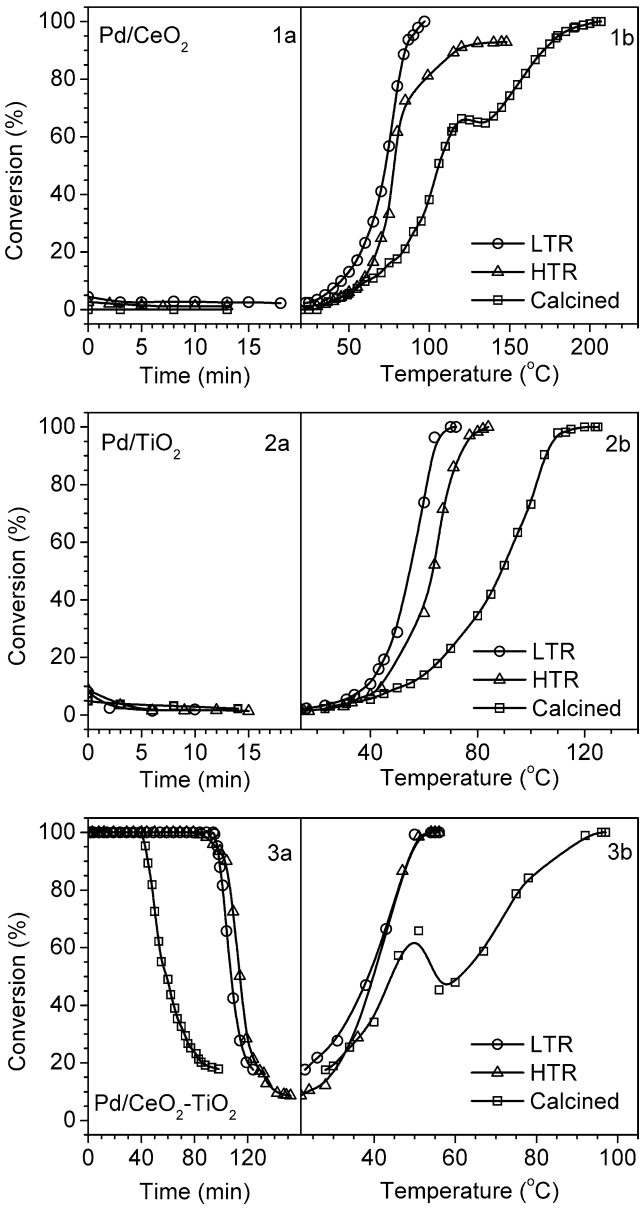

Fig. 1. Light-off profiles of CO oxidation over Pd/CeO_2 (1), Pd/TiO_2 (2), and Pd/CeO_2–TiO_2 (3) catalysts with different pretreatments: (a) activity at ambient temperature with time before heating-up, (b) CO conversion with temperature programming at a heating rate of 2 °C/min.

3.2. Pd dispersion

Metal dispersion can be achieved by selective chemisorption of probe molecules such as H_2 and CO. Because the support is able to chemisorb large quantities of H_2 (spillover) and CO for the CeO_2-containing materials even at room temperature [20–25], physical techniques such as XRD, TEM, and HTEM are also used to estimate metal dispersion [5,23, 26]. It has been found that H_2 chemisorption at 191 K [27] and CO chemisorption at 195 K [28,29] can be used as al-

ternative methods to measure the metal dispersion on ceria. Salasc et al. [30] reported that the ceria surface in contact with the precious metals could be determined by successive $O_2/H_2/O_2$ chemisorption measurements performed over Pt/CeO_2 catalysts at room temperature, which is consistent to the results obtained for H_2/O_2 titration and CO pulse adsorption. In this work, the Pd dispersion on Ce-containing catalysts was determined in similar ways.

3.2.1. Pd/CeO2

For Pd/CeO_2, because the spillover enhanced the H_2 uptake dramatically, the following chemical changes may occur in the HOT process.

H_2 chemisorption (*HC*):

$$Pd^0 + \tfrac{1}{2}H_2 \rightarrow Pd\text{–}H_{ads} \quad (H_2 \text{ adsorption on Pd, } H_{Pd}), \tag{1.1}$$

$$Ce_2O_3 + H_2 \rightarrow \overset{\text{HH}}{\text{OCe[ ]OCeO}} \tag{1.2}$$
(H_2 spilled over Ce_2O_3, S_1),

$$CeO_2 + H_2 \rightarrow \overset{\text{HH}}{\text{OCeO OCeO}} \tag{1.3}$$
(H_2 spilled over CeO_2, S_2).

O_2 titration (*OT*):

$$Pd\text{–}H_{ads} + \tfrac{1}{4}O_2 \rightarrow Pd^0 + \tfrac{1}{2}H_2O \tag{2.1}$$
(titration of adsorbed H on Pd),

$$Pd^0 + \tfrac{1}{2}O_2 \rightarrow PdO \quad \text{(oxidation of surface Pd atoms)}, \tag{2.2}$$

$$\overset{\text{HH}}{\text{OCeO OCeO}} + \tfrac{1}{2}O_2 \rightarrow CeO_2 + H_2O \tag{2.3}$$
(titration of H spilled over CeO_2),

$$\overset{\text{HH}}{\text{OCe[ ]OCeO}} + \tfrac{1}{2}O_2 \rightarrow Ce_2O_3 + H_2O \tag{2.4}$$
(titration of H spilled over Ce_2O_3),

$$Ce_2O_3 + \tfrac{1}{2}O_2 \rightarrow 2CeO_2 \tag{2.5}$$
(Ce_2O_3 oxidation or O fills in Ce_2O_3 vacancies, O_V).

H_2 titration (*HT*):

$$PdO + \tfrac{3}{2}H_2 \rightarrow Pd\text{–}H_{ads} + H_2O \tag{3.1}$$
(reduction of PdO and H_2 adsorption on Pd^0),

$$CeO_2 + H_2 \rightarrow \overset{\text{HH}}{\text{OCeO OCeO}} \tag{3.2}$$
(H_2 spilled over CeO_2),

where the symbol [ ] indicates the oxygen vacancy in the reduced CeO_2.

Then the following relations among the atomic hydrogen and oxygen consumptions may exist during these successive measurements:

$$HC = H_{Pd} + S_1 + S_2, \tag{4}$$

$$OT = 3H_{Pd}/2 + (S_1 + S_2)/2 + O_V, \tag{5}$$

$$HT = 3H_{Pd} + S_1 + S_2, \tag{6}$$

where *HC* and *HT* correspond to the hydrogen consumptions during H_2 chemisorption and H_2 titration, respectively, and *OT* to the oxygen consumption during O_2 titration; H_{Pd} is the hydrogen quantity adsorbed on Pd, which is equivalent to Pd dispersion; S_1 and S_2 correspond to the hydrogen spilled over Ce_2O_3 and CeO_2, respectively; O_V corresponds to the oxygen used to oxidize Ce_2O_3 or to fill the oxygen vacancies. All of these variables are in units of atomic μmol ratio of hydrogen or oxygen to palladium.

Based on Eqs. (4) and (6), the Pd dispersion can be attained with H_2 uptakes in the HC and HT steps by assuming that (1) hydrogen spillover for each Ce^{4+} is the same as that for Ce^{3+}; (2) no oxygen is chemisorbed on Ce^{4+}; (3) the spillover of H_2 in the HC or HT steps is not accompanied by the conversion of Ce^{4+} to Ce^{3+}, which can be deduced from the H_2-TPR [18]; (4) Ce^{3+} ions are completely oxidized to Ce^{4+} in the OT step, because it is known that Ce_2O_3 can be oxidized by O_2 at room temperature. On the basis of these considerations, Pd dispersions on the catalysts with different pretreatments are listed in Table 1.

For Pd/CeO_2 after LTR pretreatment, the apparent H/Pd ratio obtained from the HC step is 6.64, which is much higher than 1, indicating the occurrence of spillover. Through a comparison of the HC quantities of Pd/CeO_2 after different pretreatments, it can be concluded that the HTR pretreatment significantly suppresses the chemisorption of H_2 on Pd/CeO_2. However, the suppression can be recovered by OT at room temperature, and the apparent H/Pd ratio in HT is raised to 6.13, indicating a significant spillover of H_2 to ceria. Such suppression of H_2 chemisorption on Pd/CeO_2 can also be recovered by re-oxidation at 500 °C, followed by a subsequent LTR pretreatment. The Pd dispersions obtained from HOT for LTR- and ReO + LTR-pretreated samples are quite similar.

The Pd or PdO phase is not detected by XRD, and the LTR or HTR pretreatments bring little change in the particle size of the supports, as also shown in Table 1, which indicates that the sintering of Pd or supports is not evident after such pretreatments [4,5]. The suppression of H_2 chemisorption indicates the onset of SMSI induced by the HTR pretreatment, which is possibly due to the occurrence of metal decoration. As shown in Fig. 1(1b), the SMSI effects in the Pd/CeO_2 pretreated by HTR are unfavorable for CO oxidation at low temperature.

3.2.2. Pd/TiO2

For Pd/TiO_2, no evident spillover is reported, and the HOT process is predigested as follows.

HC:

$$Pd^0 + \tfrac{1}{2}H_2 \rightarrow Pd\text{–}H_{ads} \quad (H_2 \text{ adsorption on Pd}). \tag{7}$$

OT:

$$Pd\text{–}H_{ads} + \tfrac{1}{4}O_2 \rightarrow Pd^0 + \tfrac{1}{2}H_2O \tag{8.1}$$
(titration of adsorbed H on Pd),

$$Pd^0 + \tfrac{1}{2}O_2 \rightarrow PdO \quad \text{(oxidation of surface Pd atoms)}. \tag{8.2}$$

Table 1
Pd dispersion calculated from $H_2/O_2/H_2$ titration at 25 °C for the catalysts with different pretreatments

Catalyst	Pretreatment	HC (H/Pd)	HT (H/Pd)	Spilled H_2 (H/Ce)	Pd dispersion (H/Pd)	S_{BET} ($m^2\ g^{-1}$)	XRD	
							Phase	Size (nm)
Pd/TiO_2	LTR		0.92		0.31	94.1	Anatase	9.8
	HTR		0.05		0.02	80.6	Anatase	10.3
	ReO + LTR		0.91		0.30			
Pd/CeO_2	LTR	6.64	7.40	0.10	0.38	93.7	Cerianite	8.2
	HTR	0.02	6.13			87.3	Cerianite	8.1
	ReO + LTR	6.54	7.31	0.10	0.39			
Pd/CeO_2–TiO_2	LTR	0.33	0.94	0.0017	0.30	152.4	Anatase and amorphous	
	HTR	0.35	1.03	0.0006	0.34	123.4	Anatase and amorphous	

HT:

$$PdO + \tfrac{3}{2}H_2 \rightarrow Pd\text{–}H_{ads} + H_2O \quad (9)$$

(reduction of PdO and H_2 adsorption on Pd^0).

Then

$$HT = 3H_{Pd}. \quad (10)$$

The Pd dispersion is calculated from the H_2 uptakes obtained from HT based on Eq. (10), as listed in Table 1. It is noticed that the Pd dispersion of the catalysts after LTR pretreatment is higher than that after HTR; the suppression of H_2 chemisorption by HTR pretreatment is also observed on Pd/TiO_2. Such suppression can be recovered by re-oxidation at 500 °C followed by a subsequent LTR pretreatment. The suppression of H_2 chemisorption induced by HTR can also be explained by the traditional SMSI effect, which is unfavorable for CO oxidation at low temperature, as shown in Fig. 1(2b).

3.2.3. *Pd/CeO₂–TiO₂*

For Pd/CeO_2–TiO_2 with LTR pretreatment, HC (0.33) and Pd dispersion calculated from HOT (0.30) are quite similar, revealing that the spillover of H_2 on the support is not obvious. The amount of H_2 spilled over cerium oxides is only 0.0017 H/Ce, as shown in Table 1. In contrast to Pd/TiO_2 and Pd/CeO_2, no suppression of H_2 chemisorption was observed on Pd/CeO_2–TiO_2 after HTR treatment, and LTR and HTR pretreatments exhibit little difference in CO oxidation activity, as also shown in Fig. 1(3). These may imply that the nature of metal–support interactions in Pd/CeO_2–TiO_2 is different from those in Pd/TiO_2 and Pd/CeO_2. The mixed oxide may form a solid CeO_2–TiO_2 solution that hinders the decoration effect [18] and improves the reaction behavior.

3.3. *DRIFTS of CO adsorption*

The initial Pd species was determined by the spectra of CO adsorption at 25 °C after the sample was exposed to CO (5.01 vol%) in an argon flow to a saturated adsorption and then purged with a helium flow, as shown in Fig. 2. For all of the samples, the band in the region of 2300–2400 cm^{-1} is assigned to gaseous CO_2. Only Pd^0 species

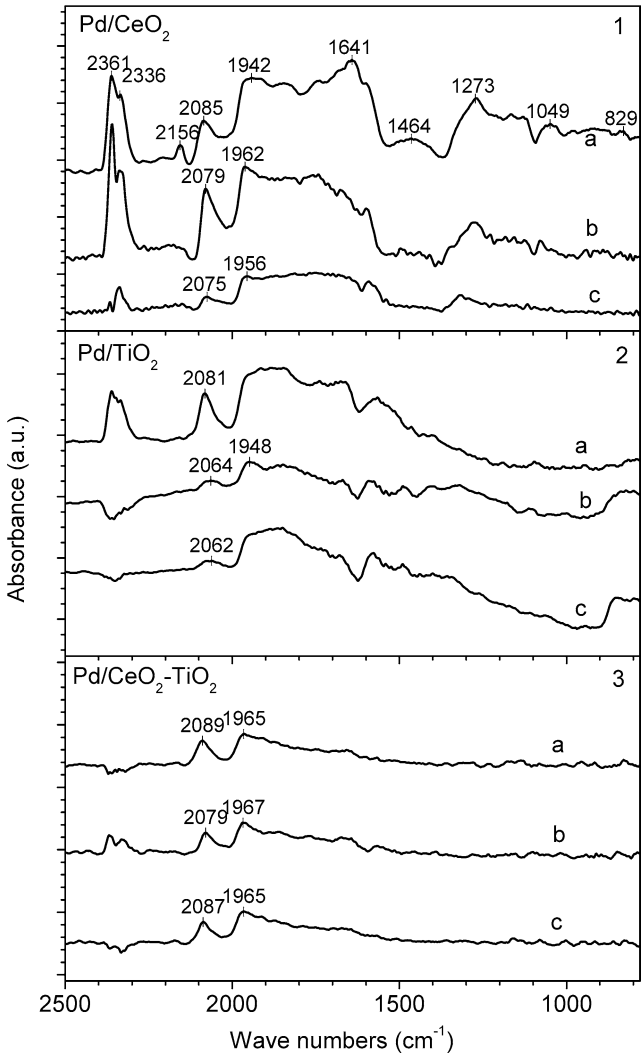

Fig. 2. DRIFTS of CO adsorption at 25 °C after purging with helium on Pd/CeO_2 (1), Pd/TiO_2 (2), and Pd/CeO_2–TiO_2 (3) with different pretreatments: (a) calcined; (b) LTR; (c) HTR.

(around 2085 cm^{-1} for linearly bonded CO and 2000–1900 cm^{-1} for bridge-bonded CO) was found in the spectra of the calcined Pd/TiO_2 and Pd/CeO_2–TiO_2, whereas Pd^{2+} (around 2156 cm^{-1} for linearly bonded CO) and Pd^0 species coexist in the calcined Pd/CeO_2, as reported previously [18].

Only the Pd^0 species was detected in the spectra of all catalysts pretreated with LTR or HTR. The intensity of CO adsorption on the HTR-pretreated Pd/CeO_2 is dramatically suppressed compared with that on the LTR-pretreated sample, which is consistent with the results of H_2 chemisorption, indicating the occurrence of the SMSI effect induced by HTR pretreatment.

The frequency of the linearly bonded CO shifts to lower wavenumbers for Pd/TiO_2 after LTR or HTR pretreatments. Meanwhile, the intensity of the adsorbed CO is also dramatically compressed, and the adsorption bands become poorly identified for the Pd/TiO_2 catalyst after reduction pretreatments; this implies a weak bond between CO and Pd for the reduced Pd/TiO_2 and the onset of the SMSI effect with the HTR pretreatment.

For Pd/CeO_2–TiO_2 with the HTR pretreatment, however, no obvious suppression of CO adsorption is observed, which agrees well with the results of H_2 chemisorption, indicating the insignificance of the SMSI effect.

It is noticeable that CO adsorption on Ce^{4+} (linearly bonded CO at 2150 cm^{-1}) or Ce^{3+} (linearly bonded CO at 2120 cm^{-1}) [28,31] is not observed in the Ce-containing catalysts, either in the calcined state or in the reduced state, which may be due to the weak adsorption of CO on Ce and/or the overlay of Ce species with Pd species.

3.4. In situ DRIFTS of CO + O_2 coadsorption

3.4.1. Pd/CeO_2

The DRIFTS of CO adsorption in (1.05% CO + 1.01% O_2)/N_2 flow at different temperatures on Pd/CeO_2 with various pretreatments are shown in Fig. 3.

The DRIFTS of the calcined Pd/CeO_2 at 25 °C shows three peaks at 2156, 2112, and 2097 cm^{-1}, which could be ascribed to the linearly bonded CO on Pd^{2+}, Pd^+, and Pd^0, respectively [32–34]. They are overlapped by the gaseous CO adsorption at 2175 and 2120 cm^{-1}. The bridge-bonded CO on Pd^0 at 2000–1900 cm^{-1} is negligible, indicating that Pd^{2+} is still the dominating species, although PdO in the calcined Pd/CeO_2 can be partially reduced into Pd species at low valence (Pd^+ and Pd^0) in the oxygen-extra atmosphere. Raising the temperature results in a continuous decrease in the intensity of carbonyls on Pd species, because of the shrinkage of CO coverage. The intensity of the bands at 2359 and 2340 cm^{-1} assigned to the gaseous CO_2 increases with the temperature, indicating an increase in CO conversion.

In the region of 1800–800 cm^{-1}, the bands at 1651, 1558, 1540, and 1506 cm^{-1} assigned to carbonate species are detected at room temperature, but the intensity depends on the temperature and shows a minimum at 80 °C and a maximum at 180 °C. The intensity variance with the temperature indicates that the carbonate species is the intermediate in the reaction. Because the PdO–CeO_2 interfacial species can be reduced by CO at 70 °C [18], it is reasonable to suggest that the reaction that occurred below 80 °C in DRIFTS measurement takes place mainly between the adsorbed CO on Pd^{2+}

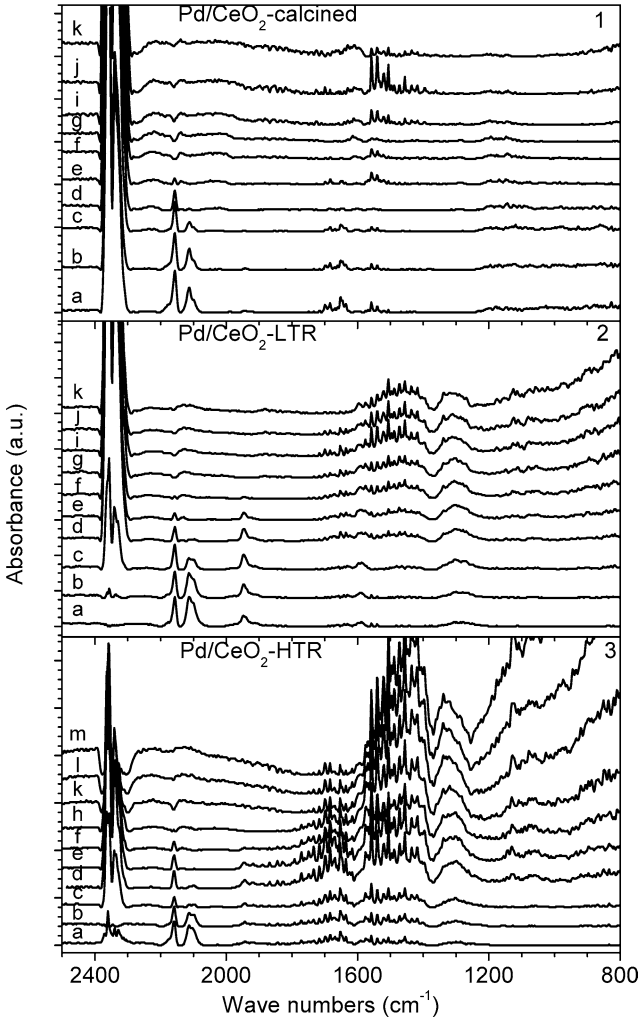

Fig. 3. DRIFTS of CO adsorption in (1.05% CO + 1.01% O_2)/N_2 flow at (a) 25, (b) 40, (c) 60, (d) 80, (e) 100, (f) 120, (g) 140, (h) 150, (i) 160, (j) 180, (k) 200, (l) 250, and (m) 300 °C on Pd/CeO_2 with different pretreatments of (1) calcination, (2) LTR, and (3) HTR.

species and the lattice oxygen of interfacial CeO_2. This reaction forms the surface carbonate intermediate, which in turn decomposes to CO_2, and the decomposition of the carbonate intermediate may be the rate-determining step. Above 80 °C, the large amounts of carbonate species present in the catalyst may cover the active sites at interfacial CeO_2 and result in a decrease in catalytic activity and a change in the reaction mechanism. It is noticeable that the adsorption of CO on Pd species cannot be detected in the DRIFTS spectra above 120 °C, which means that CO adsorption on Pd becomes weak and the adsorption of O_2 becomes noticeable. CO oxidation may then take place through the Langmuir–Hinshelwood (LH) mechanism; that is, the weakly adsorbed CO reacts with adsorbed O_2 species to produce CO_2. The intensity of carbonate species decreases when the temperature is higher than 180 °C, indicating that the decomposition of carbonate species is dramatically enhanced; thus CO oxidation may proceed via both the ceria-mediated mechanism

and the LH mechanism. These results are consistent with the light-off profiles (Fig. 1(1b)).

The DRIFTS for the LTR-pretreated Pd/CeO_2 shows that all three Pd species (Pd^{2+}, Pd^{+}, Pd^{0}) are present in the reduced samples at room temperature, indicating that Pd in the reduced Pd/CeO_2 can be partially oxidized to Pd species at high valence (Pd^{2+} and Pd^{+}) in the oxidative atmosphere. The intensity of linearly bonded CO on Pd^{+} and Pd^{0} decreases with the increase in temperature and disappears at about 80 °C. After that, the intensity of the linearly bonded CO on Pd^{2+} and bridge-bonded CO on Pd^{0} decreases with the increase in temperature and disappears above 120 °C. The results indicate that various Pd species are different in the reaction activity. The most active species is the linearly bonded CO on Pd^{+} and Pd^{0}, next is the linearly bonded CO on Pd^{2+}, and the bridge-bonded CO is the least active. The band of gaseous CO_2 appears from 60 °C, which is correlated with the light-off temperature (Fig. 1(1b)). The intensity of the carbonate species increases monotonically with the temperature, indicating that the carbonate species may be one of the products of CO oxidation on the LTR-pretreated Pd/CeO_2.

For HTR-pretreated Pd/CeO_2, all three Pd species (Pd^{2+}, Pd^{+}, Pd^{0}) are also detected at room temperature. However, the metallic Pd in the HTR-pretreated sample is much less intense than that in the calcined and LTR-pretreated samples. The bridge-bonded CO is negligible. The suppression in the intensity of the bands for adsorbed CO should be ascribed to the SMSI effect induced by the HTR pretreatment. The intensity of linearly bonded CO on Pd^{+} and Pd^{0} decreases with the increase in temperature, and the bands disappear at about 100 °C. The intensity of linearly bonded CO on Pd^{2+} decreases with temperature from room temperature to 80 °C but increases abruptly from 80 to 100 °C and then decreases again, and the bands disappear finally at 150 °C, which may indicate the presence of further conversion of Pd^{0} to Pd^{2+} in the oxidative atmosphere. Gaseous CO_2 appears from 60 °C, and the intensity increases with the temperature up to 150 °C. After that, the production of CO_2 is compressed in comparison with the LTR-pretreated sample, which implies the lower activity of the HTR-pretreated sample. Such a result is consistent with the light-off tests (Fig. 1(1b)). It is remarkable that the carbonate species is much more intense in the HTR-pretreated Pd/CeO_2 than that in the LTR-pretreated samples, which may be attributed to the fact that the carbonate species is much more stable on Ce^{3+} ions [35] and is readily produced on the migrated CeO_x species on Pd because of the SMSI effect induced by the HTR pretreatment. These may contribute to the decrease in the catalytic activity of the HTR-pretreated sample.

3.4.2. Pd/TiO_2

The DRIFTS of CO adsorption in a (1.05% CO + 1.01% O_2)/N_2 flow at different temperatures on Pd/TiO_2 with various pretreatments is shown in Fig. 4.

The DRIFTS of the calcined Pd/TiO_2 at 25 °C shows a peak at 2094 cm^{-1} that is overlapped by the bands of gaseous CO and can be ascribed to the linearly bonded CO on Pd^{0}. The bridge-bonded CO on Pd^{0} at about 1960 cm^{-1} is evident. No linear adsorption of CO on Pd^{2+} species at 2156 cm^{-1} is observed, indicating that PdO in the calcined Pd/TiO_2 is readily reduced to Pd^{0}, even in such an oxygen-rich atmosphere. The intensity of carbonate species (1800–800 cm^{-1}) increases with the temperature. A reasonable correlation is observed between the intensity of gaseous CO_2 (ca. 2350 cm^{-1}) and the light-off profiles (Fig. 1(2b)).

The spectrum at room temperature for LTR-pretreated Pd/TiO_2 shows a peak at 2095 cm^{-1}, which is ascribed to the linearly bonded CO on Pd^{0}, which was overlapped by the bands of gaseous CO at 2174 and 2118 cm^{-1}; the peak of bridge-bonded CO on Pd^{0} appears at about 1920 cm^{-1}. Pd^{2+} and Pd^{+} species were not detected in the reduced Pd/TiO_2. The adsorption of CO is compressed in comparison with

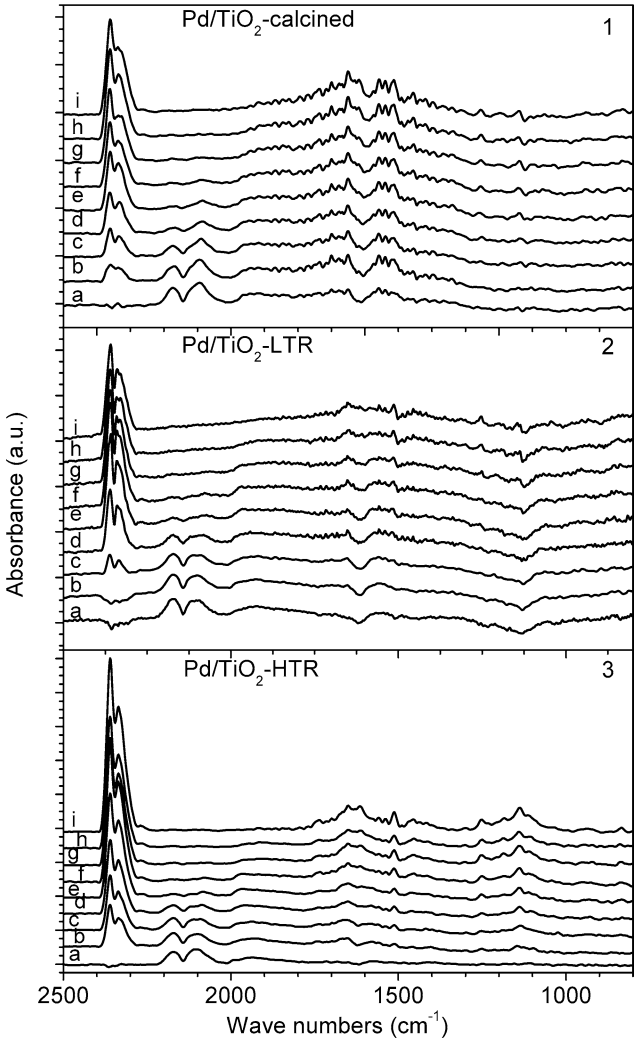

Fig. 4. DRIFTS of CO adsorption in (1.05% CO + 1.01% O_2)/N_2 flow at (a) 25, (b) 40, (c) 60, (d) 80, (e) 100, (f) 125, (g) 150, (h) 175, and (i) 200 °C on Pd/TiO_2 with different pretreatments of (1) calcination, (2) LTR, and (3) HTR.

the calcined sample. The formation of the surface carbonate species with the increase in temperature is also compressed, which may contribute to the higher catalytic activity and better stability of the LTR-pretreated Pd/TiO_2 than those of the calcined sample.

For the HTR-pretreated Pd/TiO_2, the peak of bridge-bonded CO on Pd^0 appears at 1934 cm^{-1} in the spectrum at room temperature; however, the linearly bonded CO on Pd^0 cannot be clearly identified, which is seriously overlapped by the bands of gaseous CO at 2120 cm^{-1} and results in an asymmetric peak at 2106 cm^{-1}, indicating a suppression of CO adsorption on the HTR-pretreated catalyst. The band at about 2950 cm^{-1} is visible at a temperature higher than 40 °C, which is ascribed to the C–H stretching vibration of the surface formates [31], accompanied by the appearance of the bands at 1800–800 cm^{-1} corresponding to the carbonate and formate species. The carbonate and formate species are much more intense in the HTR-pretreated Pd/TiO_2, which may also originate from the SMSI effect due to the HTR pretreatment. Unlike CO, CO_2 is easily adsorbed on TiO_2; the carbonate and formate species form on the migrated TiO_x species on Pd once CO_2 is produced.

3.4.3. Pd/CeO_2–TiO_2

The DRIFTS of CO adsorption in (1.05% CO + 1.01% O_2)/N_2 flow at 25 °C on Pd/CeO_2–TiO_2 with various pretreatments are shown in Fig. 5. The spectra of the calcined and LTR-pretreated Pd/CeO_2–TiO_2 show that only gaseous CO_2 adsorption at 2400–2300 cm^{-1} is detected without any CO adsorption, which indicates that a complete conversion of CO into CO_2 is realized at room temperature. For the HTR-pretreated samples, the bands of gaseous CO adsorption at 2170 and 2120 cm^{-1} in addition to the gaseous CO_2 adsorption are also detected; however, neither linear nor bridged CO adsorption species can be observed. The results are consistent with that of the catalytic tests (Fig. 1(3)); that is, Pd/CeO_2–TiO_2 with various pretreatments can completely convert CO to CO_2 at ambient temperature.

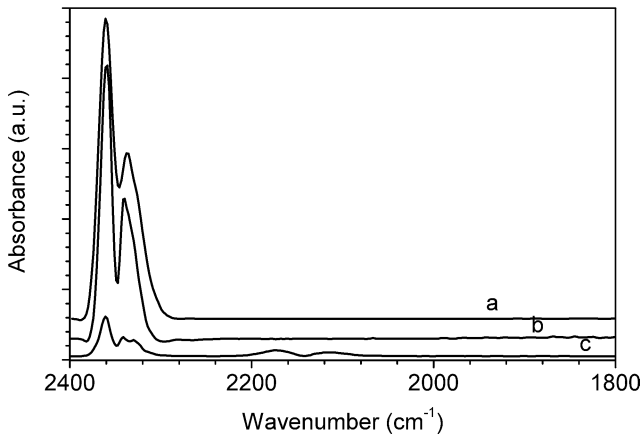

Fig. 5. DRIFTS of CO adsorption in (1.05% CO + 1.01% O_2)/N_2 flow at 25 °C over Pd/CeO_2–TiO_2 with different pretreatments of (a) calcined, (b) LTR, and (c) HTR.

3.5. Reaction mechanisms

It is generally accepted that CO oxidation on the supported noble metal catalysts proceeds via the LH surface reaction between adsorbed CO and activated oxygen [36]. The above characterizations proved that the activity of Pd/TiO_2 and Pd/CeO_2–TiO_2 is higher than that of Pd/CeO_2 [37–39], and the reduced catalysts are much more active than the corresponding calcined samples, which means that metallic Pd is more active than Pd species at higher valence. The DRIFTS and CO/H_2-TPR [18] show that PdO in Pd/TiO_2 and Pd/CeO_2–TiO_2 is readily reduced to metallic Pd under the reaction conditions, whereas Pd species at high valence (Pd^{2+} and Pd^{+}) are more stable on Pd/CeO_2 than those on Pd/TiO_2 and Pd/CeO_2–TiO_2. These may suggest that catalysts with different supports and different pretreatments are different in the reaction mechanisms for CO oxidation at low temperature.

3.5.1. Pd/CeO_2

It has been widely reported that CO oxidation over the supported noble metal catalysts could be greatly promoted by the addition of ceria [40–49]. CO oxidation over noble metal supported on CeO_2 is thought to proceed mainly through two mechanisms, that is, the mono-functional reaction path catalyzed by noble metal and the bi-functional reaction path involving the reaction between CO adsorbed on the noble metal and oxygen from ceria at the metal–ceria interface [42–44,50–52].

The mono-functional reaction path (LH mechanism) is:

$$\mathrm{CO + Pd \leftrightarrow Pd{-}CO}, \tag{11.1}$$

$$\tfrac{1}{2}\mathrm{O_2 + Pd \leftrightarrow Pd{-}O}, \tag{11.2}$$

$$\mathrm{Pd{-}CO + Pd{-}O \rightarrow CO_2 + 2Pd}. \tag{11.3}$$

The bi-functional reaction path (ceria mediated mechanism) is:

$$\mathrm{CO + Pd \leftrightarrow Pd{-}CO}, \tag{11.1}$$

$$\mathrm{Pd{-}CO + (OCeOOCeO)_s \rightarrow Pd + CO_2 + (OCeO[\ ]CeO)_s}, \tag{12.1}$$

$$\tfrac{1}{2}\mathrm{O_2 + (OCeO[\ ]CeO)_s \leftrightarrow (OCeO[O]CeO)_s}, \tag{12.2}$$

$$\mathrm{Pd{-}CO + (OCeO[O]CeO)_s \rightarrow Pd + CO_2 + (OCeO[\ ]CeO)_s}, \tag{12.3}$$

where the symbols [ ] and [O] indicate the oxygen vacancy and the oxygen activated by the vacancy, respectively.

In the current situation, Pd^{2+} is the dominant species in the calcined Pd/CeO_2, and, as proved by the DRIFTS, two mechanisms coexist in the CO oxidation reaction over the calcined Pd/CeO_2. The plateau at 120–135 °C (Fig. 1(1b)) in the light-off profile of CO oxidation on the calcined Pd/CeO_2 may be due to the alternation of the reaction mechanism, which is also reflected in the DRIFTS in situ. At low temperature, the reaction takes place mainly between the adsorbed CO on Pd^{2+} and the surface oxygen of CeO_2

(Eq. (12.1)). With the increase in temperature, the adsorption of CO on Pd^{2+} sites becomes so weak that the contribution of the reaction between adsorbed CO on Pd^{2+} and the surface oxygen of CeO_2 decreases significantly. Meanwhile, the adsorption of oxygen becomes less inhibited, which leads to the surface reaction between the adsorbed CO and O_2 (LH mechanism).

Nevertheless, Pd^{2+} site is not favorable for the activation of CO. The reduction pretreatments increase the content of metallic Pd and hence improve the activity of CO oxidation. However, the different catalytic performances cannot be attributed simply to the activity of Pd species. H_2-TPR showed that the surface CeO_2 can also be partially reduced, and thus a large number of Ce^{3+} and oxygen vacancies exist in the reduced samples to supply the active sites for oxygen (Eq. (12.2)). As a consequence, CO oxidation on the reduced catalysts may proceed mainly between CO adsorbed on the Pd sites and oxygen activated by the anion vacancies near Ce^{3+} (Eq. (12.3)).

3.5.2. Pd/TiO_2

DRIFTS and CO-TPR characterization proved that PdO in the calcined Pd/TiO_2 is partially reduced to metallic Pd with a PdO core under the reaction conditions [18]. The active sites of Pd/TiO_2 in either the calcined or the reduced form should be metallic Pd. It is generally thought that CO adsorption on the Pd-supported catalyst is so strong that the oxygen adsorption on the same sites is inhibited, which leads to the low activity of CO oxidation at low temperature [53,54]. However, the DRIFTS indicated that CO adsorption on Pd/TiO_2 is weak at ambient temperature, especially after the reduction pretreatment. Therefore, CO oxidation over Pd/TiO_2 then takes place between the weakly adsorbed CO and oxygen on metallic Pd sites through the LH mechanism, which is in agreement with the mechanisms proposed by Kochubey and Pavlova et al. [55–57].

3.5.3. Pd/CeO_2–TiO_2

Pd/CeO_2–TiO_2 catalysts with various pretreatments (calcined, LTR, or HTR) are also different in reaction behavior, which should be ascribed to the variance of the ceria state. Ceria in the calcined catalyst should be in the state of Ce^{4+}, whereas Ce^{3+} is present in the samples with LTR and HTR pretreatments.

The alteration of the reaction mechanism with temperature and the involvement of the oxygen activation at different sites were further confirmed by the catalytic behavior of the calcined Pd/CeO_2–TiO_2, where the light-off profile exhibits a peak with a CO conversion of 65% at 51 °C (Fig. 1(3b)). At low temperature, CO oxidation is mainly via the reaction between the adsorbed CO on Pd^0 sites and the lattice oxygen of surface CeO_2 at the Pd/Ce interface (Eq. (12.1)), whereas at high temperature it proceeds via the reaction between the adsorbed CO and O_2 (Eq. (11.3)).

The activity of the reduced Pd/CeO_2–TiO_2 is much higher than that of the calcined sample because of the existence of the high active Ce^{3+} and oxygen vacancies, which leads to the reaction following the bi-functional path (Eq. (12.3)).

Compared with the individual Pd/TiO_2 and Pd/CeO_2, the Pd–Ce interaction in Pd/CeO_2–TiO_2 catalysts promotes the reducibility of both PdO and CeO_2 [18] and the supply of the sites for the activation of CO and O_2 at low temperature. Over Pd/CeO_2–TiO_2, it is easier to reduce Pd^{2+} to Pd^0, which is more efficient for CO activation, and the activation of oxygen is also promoted through either the supply of surface oxygen on ceria in the calcined catalyst or the enhancement of the oxygen vacancies in the reduced sample; both factors contribute to the high activity for CO oxidation at low temperature. The reduction pretreatment enhances the metal–support interactions and gives the catalyst high activity for CO oxidation.

4. Conclusions

CO oxidation at low temperature over Pd/TiO_2, Pd/CeO_2, and Pd/CeO_2–TiO_2 with a series of calcination and reduction pretreatments was investigated in detail by catalytic light-off tests and various characterizations.

1. Pd/CeO_2–TiO_2 exhibits the highest activity among these catalysts, either in the calcined state or in the reduced state. The activity of all of the catalysts can be improved by the pre-reduction, especially by LTR pretreatment.
2. The catalysts with various supports and pretreatments are also different in their reaction mechanisms for CO oxidation at low temperature. Over Pd/TiO_2, the reaction may proceed through a surface reaction between the weakly adsorbed CO and oxygen via the LH mechanism. For Ce-containing catalysts, however, the reaction mechanism involves oxygen activation at different sites; CO adsorbed to Pd species may also interact with the surface lattice oxygen of CeO_2 or oxygen ions activated by the anion vacancies near Ce^{3+}. The distortion in the light-off profiles of calcined Pd/CeO_2 and Pd/CeO_2–TiO_2 before CO conversion achieves 100% may be ascribed to a change in the reaction mechanism with the temperature.
3. Pd dispersion determined by $H_2/O_2/H_2$ titration proves the onset of SMSI induced by the HTR pretreatment on Pd/CeO_2 and Pd/TiO_2 catalysts, which is unfavorable for CO oxidation. A CeO_2–TiO_2 solid solution may exist in Pd/CeO_2–TiO_2, which contributes to the inhibition of the decoration effect and prevents it from the suppression of H_2 chemisorption by HTR pretreatment.
4. The high activity of Pd/CeO_2–TiO_2 for CO oxidation at low temperature was probably due to the enhancements of both CO activation caused by the facilitated reduction of Pd^{2+} to Pd^0 and oxygen activation through the improvement of the surface oxygen supply and oxygen vacancy formation. The reduction pretreatment enhances

the metal–support interactions and oxygen vacancy formation and hence improves the activity of CO oxidation.

Acknowledgments

The authors are grateful for the financial support of the National Natural Science Foundation of China (20590360) and the State Key Fundamental Research Project of China.

References

[1] A. Holmgren, F. Azarnoush, E. Fridell, Appl. Catal. B 22 (1999) 49.
[2] S. Golunski, R. Rajaram, N. Hodgeb, G.J. Hutchings, C.J. Kiely, Catal. Today 72 (2002) 107.
[3] R.A. Searles, Stud. Surf. Sci. Catal. 116 (1998) 23.
[4] S.J. Tauster, S.C. Fung, R.L. Garten, J. Am. Chem. Soc. 100 (1978) 170.
[5] S. Bernal, J.J. Calvino, M.A. Cauqui, J.M. Gatica, C. Larese, J.A. Pérez Omil, J.M. Pintado, Catal. Today 50 (1999) 175.
[6] L. Fan, K. Fujimoto, J. Catal. 150 (1994) 217.
[7] L. Kepinski, M. Wolcyrz, J. Okal, J. Chem. Soc. Faraday Trans. 91 (1995) 507.
[8] J. Evans, B.E. Hayden, G. Lu, Surf. Sci. 360 (1996) 61.
[9] G.S. Lane, E.E. Wolf, J. Catal. 105 (1987) 386.
[10] R. Craciun, W. Daniell, H. Knözinger, Appl. Catal. A 230 (2002) 153.
[11] L. Kepinski, M. Wolcyrz, Appl. Catal. A 150 (1997) 197.
[12] J. Barrault, A. Alouche, V. Paul-Boncour, L. Hilaire, A. Percheron-Guegan, Appl. Catal. 46 (1989) 269.
[13] J. Cunningham, S. O'Brien, J. Sanz, J.M. Rojo, J.A. Soria, J.L.G. Fierro, J. Mol. Catal. 57 (1990) 379.
[14] G.W. Graham, H.W. Jen, W. Chun, R.W. McCabe, Catal. Lett. 44 (1997) 185.
[15] S. Bernal, J.J. Calvino, M.A. Cauqui, J.M. Gatica, C. López Cartes, J.A. Pérez Omil, J.M. Pintado, Catal. Today 77 (2003) 385.
[16] L.F. Liotta, A. Longo, A. Macaluso, A. Martorana, G. Pantaleo, A.M. Venezia, G. Deganello, Appl. Catal. B 48 (2004) 133.
[17] G.L. Dong, J.G. Wang, Y.B. Gao, S.Y. Chen, Catal. Lett. 58 (1999) 37.
[18] H.Q. Zhu, Z.F. Qin, W.J. Shan, W.J. Shen, J.G. Wang, J. Catal. 225 (2004) 267.
[19] H.P. Klug, L.E. Alexander, X-Ray Diffraction Procedures, Wiley, New York, 1967.
[20] S. Bernal, J.J. Calvino, G.A. Cifredo, J.M. Rodríguez-Izquierdo, V. Perrichon, A. Laachir, J. Catal. 137 (1992) 1.
[21] A. Bensalem, F. Bozon-Verduraz, V. Perrichon, J. Chem. Soc. Faraday Trans. 91 (1995) 2185.
[22] V. Perrichon, L. Retailleau, P. Bazin, M. Daturi, J.C. Lavalley, Appl. Catal. A 260 (2004) 1.
[23] S. Bernal, F.J. Botana, J.J. Calvino, G.A. Cifredo, J.A. Pérez-Omil, J.M. Pintado, Catal. Today 23 (1995) 219.
[24] C. Li, Y. Sakara, T. Arai, K. Domen, K.I. Maruya, T. Onishi, J. Chem. Soc. Faraday Trans. I 85 (1989) 929.
[25] C. Li, Y. Sakata, T. Arai, K. Domen, K. Maruya, T. Onishi, J. Chem. Soc. Faraday Trans. 85 (1989) 1451.
[26] S. Naito, T. Kasahara, T. Miyao, Catal. Today 74 (2002) 201.
[27] S. Bernal, F.J. Botana, J.J. Calvino, M.A. Cauqui, G.A. Cifredo, A. Jobacho, J.M. Pintado, J.M. Rodríguez-Izquierdo, J. Phys. Chem. 97 (1993) 4118.
[28] A. Holmgren, B. Andersson, D. Duprez, Appl. Catal. B 22 (1999) 215.
[29] A. Holmgren, B. Andersson, J. Catal. 178 (1998) 14.
[30] S. Salasc, V. Perrichon, M. Primet, M. Chevrier, N. Mouaddib-Moralz, J. Catal. 189 (2000) 401.
[31] G. Jacobs, L. Williams, U. Graham, D. Sparks, B.H. Davis, J. Phys. Chem. B 107 (2003) 10398.
[32] P. Chou, M.A. Vannice, J. Catal. 104 (1987) 17.
[33] K.I. Choi, M.A. Vannice, J. Catal. 127 (1991) 465.
[34] K.I. Choi, M.A. Vannice, J. Catal. 131 (1991) 1.
[35] S. Hilaire, X. Wang, T. Luo, R.J. Gorte, J. Wagner, Appl. Catal. A 215 (2001) 271.
[36] T. Engel, G. Ertl, Adv. Catal. 28 (1979) 1.
[37] M. Fernández-García, A. Martínez-Arias, L.N. Salamanca, J.M. Coronado, J.A. Anderson, J.C. Conesa, J. Soria, J. Catal. 187 (1999) 474.
[38] M. Fernández-García, A. Martínez-Arias, A. Iglesias-Juez, A.B. Hungría, J.A. Anderson, J.C. Conesa, J. Soria, Appl. Catal. B 31 (2001) 39.
[39] A. Martínez-Arias, M. Fernández-García, A. Iglesias-Juez, A.B. Hungría, J.A. Anderson, J.C. Conesa, J. Soria, Appl. Catal. B 31 (2001) 51.
[40] Y. F Yu Yao, J. Catal. 87 (1984) 152.
[41] C. Serre, F. Garin, G. Belot, G. Maire, J. Catal. 141 (1993) 9.
[42] G.S. Zafiris, R.J. Gorte, J. Catal. 139 (1993) 561.
[43] G.S. Zafiris, R.J. Gorte, J. Catal. 143 (1993) 86.
[44] S.H. Oh, C.C. Eickle, J. Catal. 112 (1988) 543.
[45] T. Bunluesin, H. Cordatos, R.J. Gorte, J. Catal. 157 (1995) 222.
[46] T. Bunluesin, E.S. Putna, R.J. Gorte, Catal. Lett. 41 (1996) 1.
[47] T. Bunluesin, G.W. Graham, R.J. Gorte, Appl. Catal. B 14 (1997) 105.
[48] A. Trovarelli, Catal. Rev. Sci. Eng. 38 (1996) 439.
[49] I. Manuel, C. Thomas, C. Bourgeois, H. Colas, N. Matthess, G. Djega-Mariadassou, Catal. Lett. 77 (2001) 193.
[50] R.H. Nibbelke, M.A.J. Campman, J.H.B.J. Hoebink, G.B. Marin, J. Catal. 171 (1997) 358.
[51] R.H. Nibbelke, A.J.L. Nievergeld, J.H.B.J. Hoebink, G.B. Marin, Appl. Catal. B 19 (1998) 245.
[52] R. Rajasree, J.H.B.J. Hoebink, J.C. Schouten, J. Catal. 223 (2004) 36.
[53] X. Zhou, E. Gulari, Langmuir 2 (1986) 709.
[54] Y.E. Li, D. Boecker, R.D. Gonzalez, J. Catal. 110 (1988) 319.
[55] D.I. Kochubey, S.N. Pavlova, B.N. Novgorodov, G.N. Kryukova, V.A. Sadykov, J. Catal. 161 (1996) 500.
[56] S.N. Pavlova, V.A. Sadykov, V.A. Razdobarov, E.A. Paukshtis, J. Catal. 161 (1996) 507.
[57] S.N. Pavlova, V.A. Sadykov, N.N. Bulgakov, M.N. Bredikhin, J. Catal. 161 (1996) 517.